Plant Physiology®

Boolink: a graphical interface for open access Boolean network simulations and use in guard cell CO₂ signaling

Aravind Karanam (1), 1 David He, 1 Po-Kai Hsu (1), 2 Sebastian Schulze, 2 Guillaume Dubeaux (1), 2 Richa Karmakar (1), 1 Julian I. Schroeder (1) 2 and Wouter-Jan Rappel (1) 1,*,†

- 1 Physics Department, University of California, San Diego, La Jolla, California 92093, USA
- 2 Division of Biological Sciences, Section of Cell and Developmental Biology, University of California, San Diego, La Jolla, CA 92093-0116, USA

These authors contributed equally (A.K. and D.H.)

W-J.R. and J.I.S. conceived and coordinated the project and analyzed the data. A.K. and D.H. created the software, ran the simulations, and analyzed the data. P-K.H. and S.S. performed the experiments. G.D. and R.K. tested the software. A.K. and W-J.R wrote the draft of the manuscript. A.K., W-J.R., and J.I.S. edited the manuscript with input from all authors.

The author responsible for distribution of materials integral to the findings presented in this article in accordance with the policy described in the Instructions for Authors (https://academic.oup.com/plphys/pages/General-Instructions) is Wouter-Jan Rappel (rappel@physics.ucsd.edu).

Abstract

Signaling networks are at the heart of almost all biological processes. Most of these networks contain large number of components, and often either the connections between these components are not known or the rate equations that govern the dynamics of soluble signaling components are not quantified. This uncertainty in network topology and parameters can make it challenging to formulate detailed mathematical models. Boolean networks, in which all components are either on or off, have emerged as viable alternatives to detailed mathematical models that contain rate constants and other parameters. Therefore, open-source platforms of Boolean models for community use are desirable. Here, we present Boolink, a freely available graphical user interface that allows users to easily construct and analyze existing Boolean networks. Boolink can be applied to any Boolean network. We demonstrate its application using a previously published network for abscisic acid (ABA)-driven stomatal closure in Arabidopsis spp. (Arabidopsis thaliana). We also show how Boolink can be used to generate testable predictions by extending the network to include CO₂ regulation of stomatal movements. Predictions of the model were experimentally tested, and the model was iteratively modified based on experiments showing that ABA effectively closes Arabidopsis stomata at near-zero CO₂ concentrations (1.5-ppm CO₂). Thus, Boolink enables public generation and the use of existing Boolean models, including the prior developed ABA signaling model with added CO₂ signaling components.

Introduction

Intracellular signaling networks are essential in almost all biological processes. These networks are often complex, involving a large number of many components (or nodes)

that are interconnected. To gain insights into these networks, it is possible to construct mathematical models. One of the strengths of these mathematical models is the ability to develop predictive outcomes of experimental

^{*}Author for communication: rappel@physics.ucsd.edu

[†]Senior author

perturbations (Phillips, 2015; Shou et al., 2015). These perturbations can be much more easily implemented in simulations than in experiments. Removing or changing a component or connection between components is a trivial task in simulations, but it is usually a task that requires lengthy wet lab experimental procedures. Predictions developed through models can enable narrowing the parameters for subsequent wet lab examinations. Wet lab examinations, in turn, can be used to iteratively update and correct mathematical models. Furthermore, mathematical models can be used to test potential biological mechanisms or to pinpoint the most important components of a signaling network (Brodland, 2015).

One way of constructing mathematical models for signaling networks is to create a rate-equation model. In such a model, the concentrations for network components can take on zero and positive rational values, and their change is governed by differential equations involving rate constants and the concentration of diverse components (Melke et al., 2006; Muraro et al., 2011; Wang et al., 2017). For example, the computational platform OnGuard can incorporate known ion transporters and channels of the guard cell network and can provide simulations of stomatal responses (Hills et al., 2012). The concentrations of soluble signaling components, however, are often not well-defined, and the strength and kinetics of many of the connections between different nodes of the network are either poorly understood or not known at all. This results in considerable uncertainty in parameter values, especially rate constants. This is particularly the case for signal transduction networks of soluble components for which rate constants are more difficult to define in a cellular context than, for example, metabolic flux networks (Feist et al., 2007).

An alternative to these "analog" networks is to formulate the problem in terms of Boolean networks (Kauffman, 1969). In these binary networks, each node can be either "ON" (1, or high) or "OFF" (0, or low) (Bornholdt, 2008; Wang et al., 2012; Schwab et al., 2020). The state of the nodes is then determined by an update rule, which involves information from the upstream nodes, and a single-time step corresponds to updating all nodes. The most commonly applied update rules are synchronous and asynchronous. For synchronous updates, the future state of each node depends on the state of the network at the current time step. In the case of asynchronous updates, the future state of a node depends on the states of nodes already updated in the current time step and on the previous states of those nodes that are not yet updated. In our application, the order of asynchronous updates is chosen in a random fashion. In Boolean networks, the regulation is no longer encoded in terms of rate constants, which may or may not be quantified by experiments, but in terms of NOT, AND, and OR logic gates. For example, in the case of an AND gate, a downstream node will be turned on (i.e. 0 transitions to 1) if and only if the upstream node is on.

Despite the significant simplification associated with the binarization, Boolean networks have been shown to be able to predict behavior in a wide variety of networks, including genetic networks (Herrmann et al., 2012; Kauffman, 1969), protein networks (Dahlhaus et al., 2016), synthetic gene networks (Zhang et al., 2014), and cellular regulatory networks (Albert et al., 2017; Lau et al., 2007; Li et al., 2004). However, the price one has to pay for the simplification is the loss of dynamic information. Moreover, the order in which the update rules are applied can critically affect the outcome of the network. Therefore, the networks are mainly used to probe the attractors of the network, defined as the states representing the long-term behavior of the system (Schwab et al., 2020).

In plants, Boolean networks have been applied to genetic networks to investigate, for example, possible crosstalk and microbe response (Genoud and Métraux, 1999; Timmermann et al., 2020). Boolean logic has also been extensively used to study ABA-induced stomatal closure in Arabidopsis (A. thaliana; Li et al., 2006; Albert et al., 2017; Waidyarathne and Samarasinghe, 2018; Maheshwari et al., 2019; Maheshwari et al., 2020). This ABA signal transduction network contains a large number of components (>80), with many unknown rate constants, and is thus challenging to encode using an analog model. In a series of studies, it was shown that the formulation of a Boolean network for ABA-induced stomatal closure was able to confirm interesting experimental data (Albert et al., 2017; Maheshwari et al., 2019, 2020). Furthermore, it was shown that the Boolean network could function as a vehicle to generate predictions. Specifically, predictions were generated through perturbations that either removed nodes or set nodes permanently to the "ON" state. Some of these predictions were subsequently tested and validated in quantitative experiments (Albert et al., 2017; Maheshwari et al., 2019).

The aforementioned studies have clearly demonstrated the potential value of casting signaling pathways into Boolean networks. However, encoding these networks, especially the ones with a large number of components, might present a significant impediment to widespread use of Boolean networks to probe, analyze, and understand signaling networks. Motivated by the challenge of creating Boolean networks that can be used by the community for independent simulations, we present in this article an opensource, user-friendly algorithm that can simulate Boolean networks, which can be easily formulated by the users. This algorithm, which we term Boolink, uses a graphical user interface (GUI) and allows the users to define nodes and their internode connections, add nodes, subtract nodes, introduce mutations, and analyze the results. Unlike other algorithms that also use GUIs, the equations are implemented in the programming language C++, which results in computationally efficient simulations. A further comparison between Boolink and existing algorithms is provided in the "Discussion". Boolink can be freely downloaded from the GitHub repository (https://github.com/dyhe-2000/BoolinkGUI or https://github.com/Rappel-lab/Boolink-GUI). User-friendly instructions for downloading and using Boolink are provided in the Supplemental data. Although Boolink can be applied to any Boolean network, we verify its use using the ABA signaling network described by Albert et al. (2017). We then describe an extension of this network that incorporates input from the stimulus CO_2 and examine the ABA-induced stomatal closing, while clamping CO_2 concentration in the leaf to very low levels (Raschke, 1975; Zhang et al., 2018). Finally, we test predictions from this extended network using quantitative experiments, and results from these experiments were used to update possible testable CO_2 input mechanisms into the network.

Results

Algorithm

Our algorithm, Boolink, simulates a Boolean network with user-defined variables and interactions. Each node of the network corresponds to a Boolean variable that can be in either of the two states: 0 (OFF) or 1 (ON). In biophysical terms, an ON state of a node corresponds to a concentration of its active form that is high enough to effect change through its interactions in the system. Conversely, an OFF state corresponds to a low concentration, which is not able to effect change. Nodes can flip their states because of their interactions with other nodes, and these interactions are encoded using an update equation. Some nodes denoting external conditions or inputs remain fixed, but affect the states of other nodes.

An update equation for a given node relates its future state to the current states of all upstream nodes. While there are several ways of formulating an update equation, our algorithm uses the so-called Sum of Products form that is intuitive and easy to formulate (Kime and Mano, 2003). This form consists of a series of terms linked by the OR logic operator. Each of these terms is a product, which contains Boolean variables connected by the AND operator. Note that these variables may be preceded by the operator NOT. A typical example used here to exemplify Boolean logic and extracted from the model of Albert et al. (2017), reads:

$$AnionEM = SLAC1 | SLAH3 \& QUAC1$$

where the symbols "|" and "&" stand for OR and AND, respectively. In this example, the future state of node AnionEM, which represents the anion efflux through the plasma membrane, is determined by the current states of three other nodes that encode two major classes of anion channels in guard cells: SLAC1, SLAH3, and QUAC1. Specifically, AnionEM is set to 1 or remains 1 if either (1) SLAC1 is 1 or (2) both SLAH3 and QUAC1 are 1 (Albert et al., 2017). In this simplification, if neither condition is met, AnionEM remains 0 or is set to 0. Using Boolink, this Boolean logic step, and any other step in the network, can be easily modified by users, and outcomes can be simulated. The Supplemental data has a brief primer on Boolean

algebra and several illustrations for formulating Boolean equations using the Sum of Products form.

In a typical simulation in Boolink, there are a few nodes that affect the nodes downstream of them but do not have any nodes upstream. As such, their states remain unchanged during the simulation. These nodes are called "input" nodes. There is typically one "output" node denoting the product or end state of the pathway, which can be monitored to determine the function of the network. For example, in the case of the ABA signaling network, ABA, Nitrite, GTP, etc., are inputs, and the output node, termed "Closure", represents stomatal closure (Albert et al., 2017). The initial states of other network nodes can be specified, based on prior knowledge, or can be assigned a random (0 or 1) value.

Once the initial states of all the nodes are specified, the program evaluates the update equations in a random order and exactly once for each node, with the output node evaluated last. The update for a single node is based on the current state of the network so that some of its upstream nodes may already have been updated in the same time step. This so-called asynchronous updating is motivated by the fact that many of the reaction rates are unknown, resulting in nondeterministic outcomes. A single-time step in the simulation corresponds to each node being updated once. The number of time steps, corresponding to one iteration over all the nodes, can be chosen by the user and should be large enough for the system to reach a steady state. Furthermore, the user also specifies the number of simulations, each with randomly chosen initial conditions. All parameters, equations, and initial conditions can be easily entered into Boolink using an intuitive graphical interface. Finally, Boolink is able to display graphs of the dynamics of one or more nodes, and all variables are stored for later analysis.

Simulations

Boolean network introductory and training example

As a first example, we investigate a very simple Boolean network, shown in Figure 1A. This network contains an input node (IN), an output node (OUT), and three intermediate nodes X, Y, and Z. The input node does not depend on any other nodes, which is simply written as IN = IN. Furthermore, X and Y reinforce each other, and X inhibits Z through a NOT link (denoted by the symbol \sim in the equations and flat arrowheads in Figure 1A), while IN inhibits X; Y inhibits OUT and Z activates OUT. For both X and OUT, the two inputs combine according to the AND logic as denoted by a "&". The Boolean update equations can thus be simply written as follows:

$$\begin{split} \text{IN} &= \text{IN} \\ \text{X} &= \text{Y\&} \sim \text{IN} \\ \text{Y} &= \text{X} \\ \text{Z} &= \sim \text{X} \\ \text{OUT} &= \sim \text{Y\&Z} \end{split}$$

The dynamics of this network can be worked out by hand or, since it only contains three nodes, can be analyzed

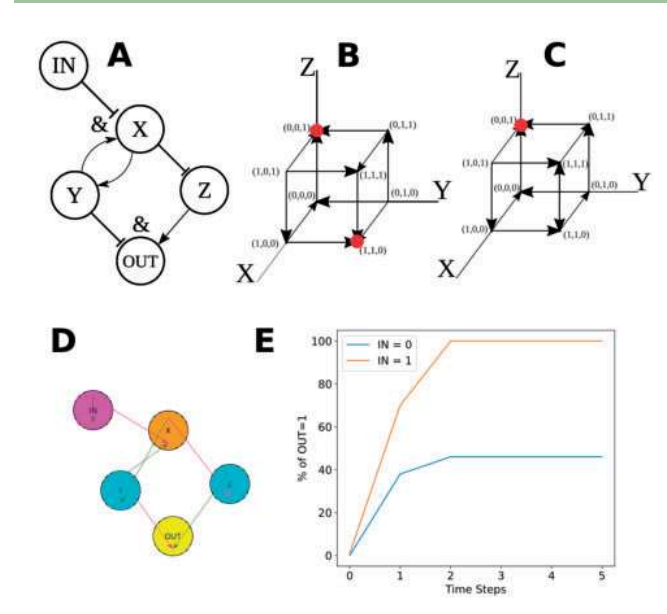


Figure 1 Simple Boolean network and its implementation into Boolink. A, Schematic of the network. Pointed arrowheads indicate positive regulation and flat arrowheads indicate negative regulation. For nodes X and OUT, the two inputs combine using AND logic, indicated by the symbol '&'. B, State space and dynamics, represented by arrows, in the absence of input (IN = 0). The two possible attractors, (0,0,1) and (1,1,0), are indicated by red dots. C, State space and dynamics in the presence of input (IN = 1). The only attractor, (0,0,1), is indicated by a red dot and leads to OUT = 1. D, Representation of the Boolean model in the Boolink GUI. Green and magenta arrows indicate positive and negative regulation, respectively. An arrow within the node indicates self-regulation. In this representation, one can "search" for upstream and downstream nodes of a given node. Here, X (colored in orange) has two downstream nodes, colored in cyan, and one upstream node, colored in magenta. Other node(s) are colored in yellow. E, Percentage of OUT = 1 versus time step in an asynchronous update scheme starting with randomly assigned initial states for the intermediate nodes when the input is present (IN = 1, orange line) and absent (IN = 0, blue line).

graphically. One feature of an asynchronous update scheme is that the updated state is always the "nearest neighbor" of the previous state. Therefore, the evolution of the states can be represented as a continuous trajectory through the state space, with dimensions equal to the number of nodes. This is shown in Figure 1, B and C, for our simple model in the absence (IN = 0; B) and in the presence of input (IN = 1; C). The 3D state space is spanned by X, Y, and Z, and all possible states of the intermediate nodes are points in this 3D space that are connected by arrows according to the rules of the Boolean network. By following these arrows, the attractors for the model can be determined. For example, in the absence of input (Figure 1B), the state X = 1, Y = 0, and Z = 0, compactly written as (1,0,0), can transition to either (0,0,0) or (1,1,0). Since no arrows originate from (1,1,0), this is an attractor of the system: this state will remain unchanged indefinitely. Furthermore, the only permissible transition from (0,0,0) is to (0,0,1), which can easily be seen as an attractor as well. Since only (0,0,1) leads to the ON state of the OUT node, we find that OUT = 1 in 50% of the possible initial conditions. However, in the presence of input (IN = 1), it is easy to verify that the only possible attractor is (0,0,1), and thus, OUT = 1 for all initial conditions. Calculations and further analysis on this simple network are provided in the Supplemental data.

The implementation in Boolink is shown in Figure 1D, obtained after specifying the input files in the subfolder "sample_data_files/simple_network_data_files" of the repository (https://github.com/dyhe-2000/Boolink-GUI or https:// github.com/Rappel-lab/Boolink-GUI). Here, the green/magenta arrows indicate positive/negative regulation and an arrow within the IN node indicates self-regulation. In Boolink, all nodes are visualized in yellow by default. However, connections between a particular node and other network nodes can be easily visualized by double-clicking on the specific node, after which it changes its color to orange. Upstream nodes will then change their color to magenta, while downstream nodes will turn cyan. In the example of Figure 1D, this procedure has been carried out by clicking on node X. Note that the color scheme for the nodes can be changed by the user. (See Supplementary data section 2, "Downloading and Running Boolink".)

This network was simulated using Boolink, choosing five time steps and 50 different sets of initial conditions. The results of these simulations are shown in Figure 1E, where we plot the state of the output node, expressed as the percentage of runs in which OUT = 1, in the absence (blue line, IN = 0) and presence (orange line, IN = 1) of input. Note that time in these plots indicates the iteration number. The state of the simulation that is of physiological relevance is the steady state; here it is reached after two steps. Consistent with the arguments presented above, the simulations show that this percentage is 50% when IN = 0 and 100% when IN = 1.

ABA network

Next, we applied Boolink to the ABA-induced stomatal closure network formulated by Albert et al. (2017). The input file for this network, containing all components by name and their interactions, can be found in the subfolder "sample_data_files/ABA_data_files/" of the repository for the Boolean equations and for the names of the nodes (https:// github.com/dyhe-2000/Boolink-GUI or https://github.com/ Rappel-lab/Boolink-GUI). The reconstruction of the published ABA signaling network (Albert et al., 2017), within the Boolink interface here, will enable any user to use and manipulate components of this network and develop experimental predictions and to modify the Boolean network depending on experimental outcomes or to predict outcomes for modified network models. A screenshot of our implemented network encoded within the Boolink GUI is presented in Figure 2, with the input ABA node shown in red and the "Closure" output node shown in green. This network contains 81 nodes, including input and output nodes, and was constructed by and adapted from Albert et al.

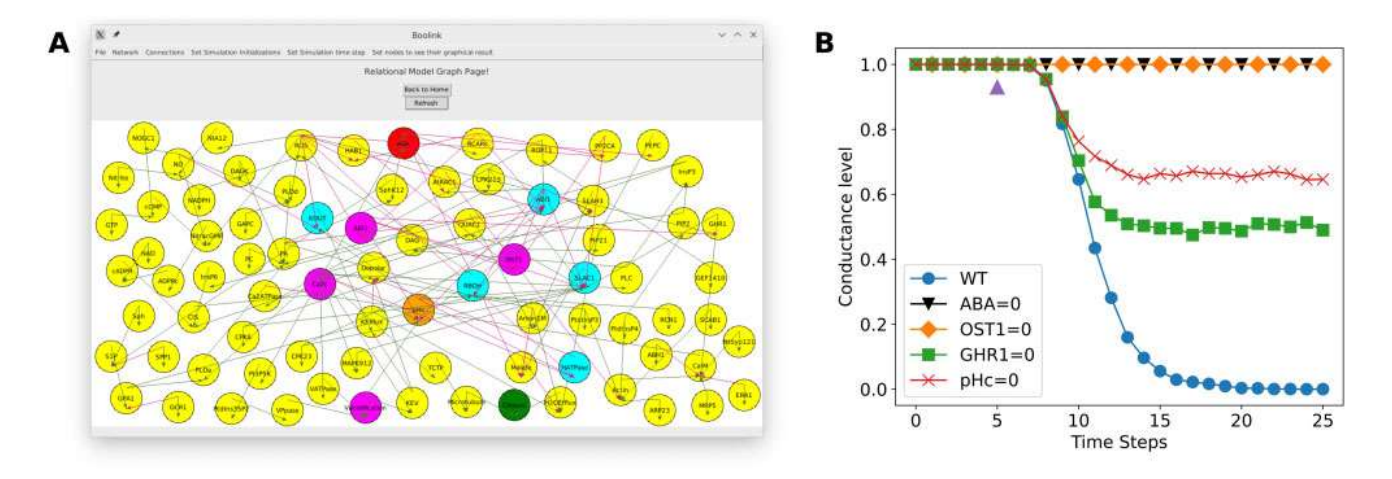


Figure 2 Implementation of ABA signaling into Boolink A: Visualization of the Boolean network for ABA-induced stomatal closure (Albert et al., 2017), rendered here by the Boolink GUI. The input ABA and output Stomatal Closure are colored in red and green, respectively. The node denoting cytoplasmic pH (pHc), colored in orange, has its upstream nodes colored in magenta and downstream nodes in cyan. Connections for any node can be viewed by double-clicking on the node of interest (see Results). B: Simulated stomatal conductance as a function of time steps in the simulation for wild type (with and without ABA) and the mutants ost1 and ghr1, and alteration of cytosolic pH (pHc) based on the model of Albert et al. (2017) (see Results). A conductance level of 1 corresponds to maximal relative stomatal conductance while 0 represents complete stomatal closure. The violet triangle shows the point in the simulation where ABA is introduced (except for the case ABA=0).

(2017) following an extensive survey of more than 100 peer-reviewed articles. As in the simple example, the interactions between nodes in the GUI are color-coded, with green arrows representing positive interactions and magenta arrows representing negative interactions. Using the Boolink GUI, the user can move nodes around by simply dragging them to a new location. Furthermore, to facilitate examining internode connections, double-clicking on a node reveals all downstream and upstream interactions of that node (Figure 2A). (See https://github.com/dyhe-2000/Boolink-GUI or https://github.com/Rappel-lab/Boolink-GUI; detailed instructions can be found in the Supplemental data).

Results of the Boolink simulations for 25 time steps and averaged over 2,500 initial conditions are presented in Figure 2B. In this and subsequent curves, following Albert et al. (2017), we chose to illustrate the predicted stomatal conductance level as a function of simulation (time) step. However, and as discussed above, this time step does not equate to "real time", and only the steady state following a change in network architecture or input can be compared to experimental results. This conductance level, computed as 1-Closure, varies between 0 (corresponding to closed stomata and Closure = 1) and 1 (corresponding to open stomata and Closure = 0) and facilitates comparison with experiments in which the stomatal conductance is presented (Figures 3 and 4). In the absence of ABA, simulated by setting the input node ABA to 0 throughout the simulation, the output node Closure is 0 for all time steps, corresponding to no stomatal closure and a conductance level of 1 (black triangle curve). In the presence of ABA, modeled by changing ABA from 0 to 1 at time step five, the network reaches a conductance level of 0 (stomatal closure) after approximately 15 time steps (blue curve, labeled as wild-type [WT]). By implementing the model of Albert et al. (2017),

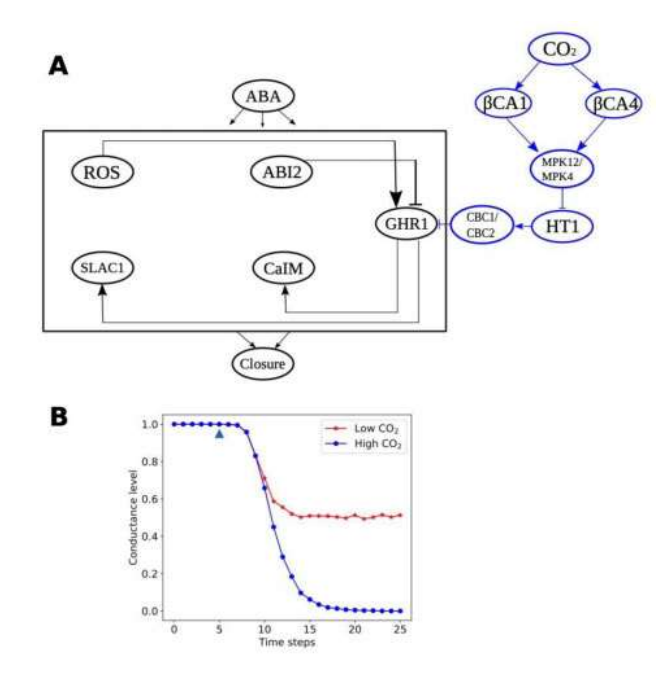


Figure 3 Stomata 2.0 and Boolink. A, ABA-driven stomatal closure model extended with a CO_2 branch, indicated in blue, which positively regulates GHR1. The box denotes all the intermediate nodes of the original ABA network shown in Figure 2, with only GHR1 and its immediate upstream and downstream nodes shown. B, Predicted relative stomatal conductance levels obtained by implementing Stomata 2.0 into Boolink for two concentration levels of CO_2 : low ($CO_2 = 0$; red line and symbols) and high ($CO_2 = 1$; blue line and symbols). The triangle shows the point in the simulation where ABA is introduced (ABA = 1).

we have also computed the relative stomatal conductance for several mutants, labeled in Figure 2B, following the introduction of ABA after five time steps. Knocking out the

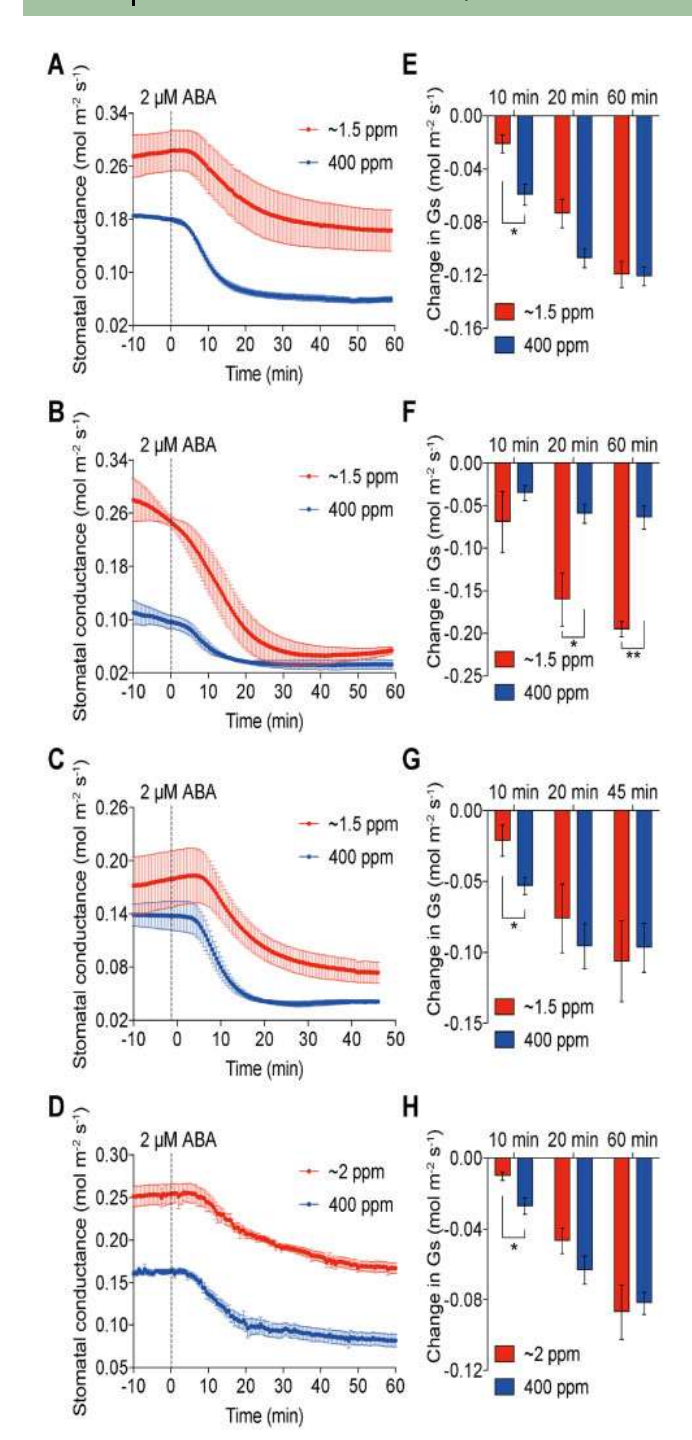


Figure 4. ABA-mediated stomatal closing responses of WT leaves during CO_2 "starvation". A–C, Intact excised leaves of WT plants (n=3 to 4 independent leaves per treatment and experimental set) were equilibrated at 400 ppm CO_2 or \sim 1.5 ppm CO_2 for 60 min prior to stomatal conductance measurements. Stomatal conductances were measured with a LI-6400XT Portable Photosynthesis System. D, Timeresolved stomatal conductance responses to ABA in intact excised leaves (n=5 independent leaves per treatment) equilibrated at \sim 2 ppm CO_2 or 400 ppm CO_2 for 2 h prior to ABA application. Experiments were carried out using a LI-6800 Portable Photosynthesis System. In each experimental set, 2- μ M ABA was applied through the transpiration stream via the petiole at time = 0 min. CO_2 concentrations in the intercellular spaces of leaves (Ci) equilibrated under CO_2 starvation were computed using the gas exchange analyzer (see

Open Stomata 1 (OST1) protein kinase, which corresponds to forcing the node OST1 to 0 at all times, results in a conductance level that remains 1 (no stomatal closure) after setting ABA = 1 (orange diamond curve). Furthermore, knocking out guard cell hydrogen peroxide resistant 1 (GHR1) results in a conductance level of 0.5 (50% stomatal closure) following the introduction of ABA (green square curve) and manipulating the cytosolic pH through the node pHc leads to a conductance level of approximately 0.65 (red X curve). These control predictions are identical to the ones obtained in the original publication (Albert et al., 2017), further validating reconstruction of this network in our interactive graphical user interface.

CO2 network

We next applied our GUI to examine and explore the guard cell signaling network. We used the original ABA network of Albert et al. and first extended it with a putative branch that models the input of CO₂. Elevated CO₂ triggers stomatal closure and some elements of CO₂ signaling overlap with those of ABA signaling, whereas others affect stomatal closure through separate pathways (Hsu et al., 2018; Merilo et al., 2015; Zhang et al., 2020). Based on previous experimental data, we modeled the CO₂ branch to be upstream of GHR1 in the ABA network (Horak et al., 2016; Jakobson et al., 2016). The added branch contains CO₂ as input, which is then catalyzed by the beta carbonic anhydrases BCA4 and β CA1 in parallel (Hu et al., 2010, 2015). These then activate the node Mitogen-Activated Protein Kinase 4 and 12 (MPK4 and MPK12) via mechanisms that are yet unknown. This node inhibits the negative-regulator of CO2-induced stomatal closing, the high temperature 1 (HT1) protein kinase, which, in turn, regulates the convergence of blue light and CO₂ 1 and 2 (CBC1 and CBC2) protein kinases either directly or indirectly (Hashimoto et al., 2006; Horak et al., 2016; Hiyama et al., 2017). Finally, CBC1/CBC2 enters the ABA network through an assumed inhibitory link to GHR1 (Figure 3A).

The above summarized CO₂ branch can be translated into the following Boolean equations:

$$\begin{aligned} \text{CO}_2 &= \text{CO}_2 \\ \beta \text{CA1} &= \text{CO}_2 \\ \beta \text{CA4} &= \text{CO}_2 \\ \text{MPK12/MPK14} &= \beta \text{CA4} | \beta \text{CA1} \\ \text{HT1} &= \sim \text{MPK12/MPK14} \\ \text{CBC1/CBC2} &= \text{HT1} \\ \text{GHR1} &= \sim \text{ABI2\&ROS\&} \sim \text{CBC1/CBC2} \end{aligned}$$

Note that the equation for GHR1 is adapted from Albert et al. and takes into account the existing connections from

"Materials and methods"), with Ci values <20 ppm (A–C) and <3 ppm (D) before application of ABA. E–H, Changes (differences) in stomatal conductance at the indicated time points after ABA application compared to 0 min. Data present mean \pm sem. *P < 0.05 and **P < 0.01 Student's t test in E–H.

the ABA network (from ABI2 and ROS) and the new input from the CO₂ branch. This simplified CO₂ signaling model, which can be accessed in the online Boolink repository, termed Stomata 2.0, includes presently identified and confirmed early CO₂ signaling mechanisms that have been found to function in the CO₂ signaling pathway upstream of the merging with the ABA-induced stomatal closing pathway (Hsu et al., 2018; Zhang et al., 2018, 2020).

Based on this model, we then determined how the extended network responds in simulations to ABA under high and low CO₂ conditions (Figure 3B), simulated by setting the input node for CO₂ to either 0 (very low concentration) or 1 (high concentration) and again averaging over 2,500 initial conditions. For $CO_2 = 1$, the introduction of ABA at time step five results in a decrease of conductance level from 1 to 0 (Figure 3B, blue curve), identical to the WT response shown in Figure 2 (blue curve). This can be understood as the added CO₂ branch having little or no effect on the ABA network since CBC1/CBC2 is 0 when $CO_2 = 1$. Note that in this model, the starting steady-state stomatal conductance of 1 is similar at each background CO₂ concentration, which will be addressed in updated simulations further below. When simulating very low CO2 conditions, our simulations predicted that introduction of ABA also induces stomatal closure and, thus, a decrease in the conductance level. However, the ABA-induced conductance level in the presence of low (nominally 0) CO2, was found to be reduced from 1 to 0.5 (Figure 3B, red curve).

To test our predictions experimentally, we analyzed ABA-mediated stomatal closure under either 400 ppm or near-zero ppm (\sim 1.5 ppm) CO₂ by conducting gasexchange experiments with ABA application to the transpiration stream of excised intact leaves (Ceciliato et al., 2019). Our results showed that application of 2-µM ABA induced robust stomatal closure in leaves exposed to 400-ppm CO₂ as expected (Figure 4, A-D, blue curves). As stomatal responses are known to show biological noise, and as ABAinduced stomatal closing in Arabidopsis spp. has not been previously analyzed at near-zero CO2, we conducted four independent sets of experiments (Figure 4). In all four experiments, leaves exposed to 1.5-ppm CO₂ showed robust stomatal closing in response to 2-µM ABA, with a degree of expected biological variation (Figure 4, A-D, red curves). By analyzing the steady-state stomatal conductance in leaves, it appears that the response to ABA at low CO2 was reduced in three of these experiments (Figure 4, A, C, and D). We also compared the difference (change) in steady-state stomatal conductance before and after applying ABA (Figure 4, E-H). This analysis shows that independent of whether leaves are exposed to 400-ppm CO₂ or 1.5-2-ppm CO₂, the ABA responses had a similar magnitude in three of the experiments, and there was a stronger ABA response in one of the experiments (Figure 4F). Furthermore, our data show that in the absence of ABA, leaves exposed to low CO2 show a higher stomatal conductance than leaves exposed to 400-ppm CO₂. This is consistent with a reduction in stomatal conductance upon CO_2 elevation. In addition, analyses of an early time point of the ABA response, 10 min after ABA addition, show a slightly, but significantly, slowed initial ABA response in three of four experiments when compared with controls exposed to 400-ppm ambient CO_2 (Figure 4, E, G, and H). Taken together, our experimental data show that the steady-state stomatal conductance responses to ABA in Arabidopsis remain, to a large degree, intact even at very low, near-zero CO_2 concentration and as an approximation indicate a steady-state additive effect of low CO_2 on the stomatal conductance prior to ABA exposure.

A comparison of our experimental results and model predictions in the absence of ABA reveals that Stomata 2.0 (Figure 3B) is not able to fully capture the dependence of the steady-state conductance levels on CO2. This suggests that additional modifications of the ABA network are required to reproduce the observed reduction of stomatal conductance in the presence of CO₂. To explore possible modifications that result in model predictions that are more consistent with our experimental steady-state response results, we utilized the ability of Boolink to easily modify, simulate, and visualize modified Boolean network outcomes. We found that we were able to better reproduce experimental data if we modified the Boolean equations for four network components (Figure 5A). Specifically, we modified the nodes cytosolic calcium (Ca2c), which is linked in the ABA model (Albert et al., 2017) to Ca²⁺ influx across the plasma membrane (CaIM), microtubule depolymerization (microtubule), and water efflux through the plasma membrane (H2OEfflux) to:

```
\begin{split} \text{Ca2c} &= \sim \text{Ca2ATPase \& (CIS | CalM) } | \underline{\text{(ABA\&CO}_2\text{)}} \\ \text{CalM} &= \sim \text{ABH1 \& (NtSyp121 | MRP5 | GHR1) } | \sim \text{ERA1 | Actin } | \underline{\text{CO}_2} \\ \text{Microtubule} &= \text{TCTP | Microtubule \& } \underline{\text{ABA}} \\ \text{H2OEfflux} &= \text{AnionEM \& PIP21 \& KEfflux \& } \sim \text{Malate } | \text{CO}_2 \\ \end{split}
```

where the modifications are underlined. Introducing a CO₂ dependence on calcium signaling was motivated by experimental evidence that Ca2c was involved in CO2-induced stomatal closure (Webb et al., 1996; Schwartz et al., 1988; Schulze et al., 2021). Furthermore, findings that anion efflux and water efflux functions in the CO2 response and that GHR1 functions in CO2-induced stomatal closure were included (Horak et al., 2016; Jakobson et al., 2016). Addition of an ABA component to microtubule function was motivated based on recent findings (Rui and Anderson, 2016; Qu et al., 2018). These modifications, their associated Boolean logic operations, and their effect on stomatal closure are further detailed in the Supplementary data. When simulating this modified and updated network, termed Stomata 2.1, we found that the steady-state conductance level now depends on CO₂ and is reduced for high CO₂ conditions (Figure 5B). Furthermore, and also approximately consistent with the experiments, the introduction of ABA reduces stomatal conductance by similar absolute conductance changes for both low and high CO₂ conditions (Figure 5B). The Stomata 2.1 network is able to reproduce experimental results better.

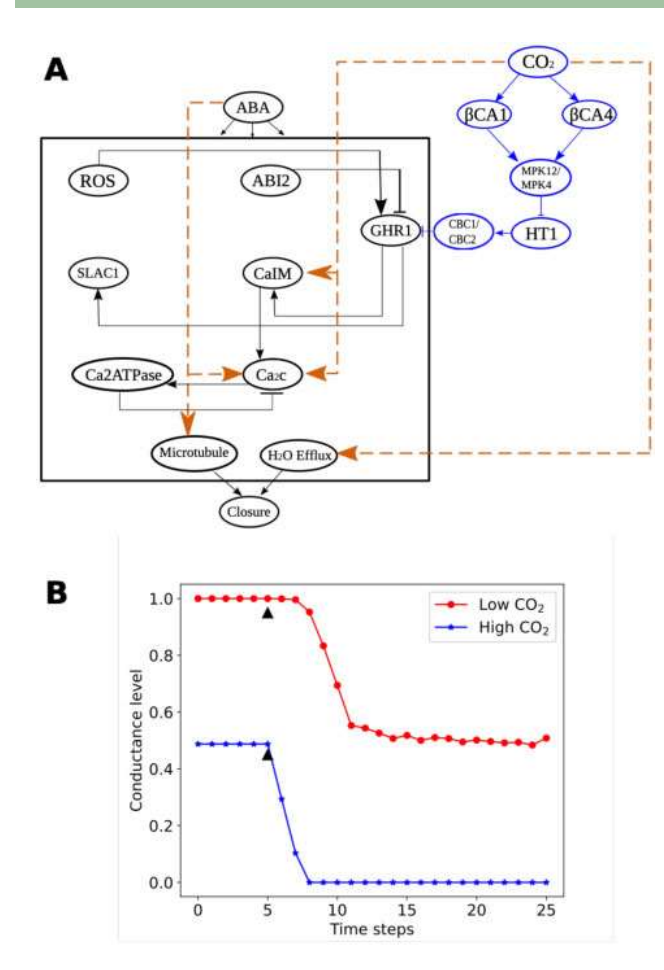


Figure 5. Stomata 2.1 and Boolink. A, ABA-driven stomatal closure model extended with a CO_2 branch, indicated in blue, which positively regulates GHR1, and additional modifications represented by the orange links (read the study for details). B, Predicted relative stomatal conductance levels obtained by implementing Stomata 2.1 into Boolink for two concentration levels of CO_2 : low ($CO_2 = 0$; red line and symbols) and high ($CO_2 = 1$; blue line and symbols). The triangle shows the point in the simulation where ABA is introduced.

We have included the network files for both Stomata 2.0 and 2.1 in the folder "sample_data_files/in the Boolink repositories". We anticipate that community members will be able to use Boolink as a starting point to easily introduce modifications and iteratively test predictions.

Discussion

Large signaling networks are common in biology, in general, and plant physiology. The published ABA signaling network we implemented into Boolink, for example, contains more than 80 components (Albert et al., 2017). The vast majority of the interaction strengths and kinetic parameters between these components are not known, making it difficult to formulate mathematical models of these networks. Motivated by the simplicity and utility of Boolean networks and the challenges associated with formulating detailed rate equation-based models for these large networks, we have presented here a software package with a GUI that can simulate, visualize, and plot the results of a user-defined

Boolean network. Our package, named Boolink, is free to use and distribute and is built from free and open-source software. The interface is intuitive, and users do not require extensive coding knowledge to use it. The Supplementary data contains detailed instructions on downloading, installing, and running Boolink on Windows, Mac, and Linux-based machines. In addition to this open-source version, we also packaged the software in a "Docker container", which allows execution of Boolink in an even more facile and direct computer operating system-independent fashion. Instructions on how to obtain the Docker container is also provided in the Supplementary data.

Boolink platform and advantages

As reviewed by Schwab et al. (Schwab et al., 2020), a number of computational platforms exist that are able to simulate Boolean networks and can be useful in certain applications. Boolink, however, is distinct from these platforms for several reasons, making it uniquely capable of analyzing the large-scale Boolean networks addressed in this study. First of all, many of the existing packages, including BoolSim (Garg et al., 2008), ChemChains (Helikar and Rogers, 2009), MaBoSS (Stoll et al., 2012), Pint (Paulevé, 2017), BooleanNet (Albert et al., 2008), BoolNet (Müssel et al., 2010), and PyBoolNet (Klarner et al., 2017), do not use GUIs and cannot visualize the network. Obtaining an intuitive understanding of networks without a graphical interface becomes increasingly difficult as the number of nodes increases. Furthermore, having the Boolink GUI allows users to determine connections between nodes with a simple click on the graphical representation. Furthermore, the packages SQUAD (Di Cara et al., 2007), SimBoolNet (Zheng et al., 2010), and Polynome (Dimitrova et al., 2011) either are no longer available or use Java versions that are no longer supported. In addition, CellNetAnalyzer (Klamt et al., 2007), is implemented in MATLAB and is, thus, not open source. Also, BooleSim (Bock et al., 2014) and CellNOptR (Terfve et al., 2012) only use synchronous updating and cannot implement the evaluation of nodes in an asynchronous order. Finally, ViSiBool (Schwab and Kestler, 2018), GINsim (Gonzalez et al., 2006), and The Cell Collective (Helikar et al., 2012) can only run a single initialization at a time. This means that performing the computational studies reported in Figures 3 and 4, which used 2,500 randomly chosen initial conditions, would require manually starting 2,500 separate simulations.

To further distinguish Boolink from existing packages, we have performed a benchmarking study to compare the computational efficiency of our platform with that of two existing packages, GINsim and The Cell Collective, that are GUI-based, are open source, can perform asynchronous updating, and can plot results. Both of these packages are implemented using Java, which can be expected to be less efficient than our C++-based platform (Hundt, 2011; Prechelt, 2000). To benchmark GINsim, we used a published Boolean network comprising 18 nodes that models the cellular cycle in budding yeast (Irons, 2009). Computing 2¹⁸

asynchronous updates for all possible states of this network took 35.83 s in GINsim. Simulating the same network in Boolink and for 50 time steps and 2,500 initial conditions, corresponding to $2500*50*18 = 2.25 \times 10^6$ asynchronous updates, took 8.2 s. Comparing the Central Processing Unit (CPU) time per update reveals that Boolink is faster than GINsim by a factor of 38: 3.64×10^{-6} s per update versus 1.37×10^{-4} s per update. To benchmark The Cell Collective, we simulated our simple five-node network (Figure 1) for one initialization and 10,000 time steps. This simulation required approximately 1 min and 45 s or around 0.01 s per time step using The Cell Collective. In contrast, Boolink was able to complete this simulation in 0.338 s, with a difference in speed of approximately 340. This considerable advantage in computational efficiency can become particularly attractive for large-scale networks that need to be run multiple times, as is the case for our CO₂ signaling network. Coupled to a user-friendly graphics interface, our C++ implementation should thus provide a fast and userfriendly platform for the exploration of Boolean networks. Furthermore, our platform is independent of operating system and can be installed on Linux, Windows, and Mac operating systems. The explicit instructions and the Docker container we provide should facilitate this installation.

Boolink uses asynchronous and random order of updates, which is best suited to simulate a network of chemical reactions in which the outcome of one reaction then affects the outcome of another in the near future (hence asynchronous), and when the relative rates of different reactions in the network are unknown (hence random order of update). Besides nodes and connections, users may also specify the number of time steps or iterations to run the simulations and the number of initial conditions to get a statistically robust sample output. Once a system is defined, it may be visualized as a network in Boolink. Visualization includes identifying the upstream and downstream nodes of a given node and the type of connections (activating or inhibiting) between them, by simply double-clicking on the node of interest. The steady states of nodes of the system after simulation can be quickly plotted within Boolink. The trajectory of the entire simulation is stored in a NumPy array; a Jupyter notebook is provided with the package, which can be used to further analyze the system starting from the NumPy array, including producing publication-ready plots of the simulation.

Guard cell CO₂ signaling iterative modeling

We first tested and verified Boolink using a published advanced model for stomatal closure in guard cells as mediated by ABA and verified that our simulations were consistent with those of Albert et al. (2017). We then extended the network to include the effects of CO₂ on stomatal movements. Previous research indicated that CO₂ might mediate signal transduction via the OST1 protein kinase, as ost1 mutant leaves were impaired in their stomatal response to CO₂ elevation (Merilo et al., 2013; Xue et al., 2011). However, more recent studies unexpectedly showed that, in

contrast to ABA, CO₂ elevation does not activate the OST1 protein kinase (Hsu et al., 2018; Zhang et al., 2020). This research further provided experimental evidence that basal OST1 protein kinase activity and basal ABA signaling are required for WT-like CO₂-induced stomatal closure (Hsu et al., 2018; Zhang et al., 2020; Figures 3 and 4). Thus, merging CO₂ signaling into the extant ABA signaling model is reasonable. The biochemical link by which CO₂ signaling merges with ABA signaling is proposed to lie downstream of the OST1 protein kinase but remains unknown. In the present study, to test a simplified model merging the ABA signaling and CO₂ signaling networks, we modeled this link to occur at the level of the transmembrane receptor-like (pseudo)kinase GHR1 (Hua et al., 2012; Sierla et al., 2018).

The simulations of this simplified network predicted that the response to ABA should depend on the CO₂ concentration (Figure 3). This prediction was then subsequently analyzed, and ABA-mediated stomatal closure of intact Arabidopsis spp. leaves was measured while leaves were either exposed to ambient 400-ppm CO₂ or near-zero (1.5 ppm) CO₂ (Figure 4). Interestingly, our data show that leaves exposed to 1.5-ppm CO₂ exhibited a robust response to ABA. Under low CO2 conditions, the stomatal conductance remained higher prior to ABA application at a steady state than at 400-ppm CO₂ (Figure 4A). When comparing true steady-state stomatal conductance responses, it appears that CO2 and ABA may in part have additive responses in Arabidopsis as a first-order approximation. (Note that basal ABA signaling amplifies or accelerates the CO₂ response [Hsu et al., 2018], such that the starting stomatal conductance was much higher at low CO₂ due to the lack of CO₂induced stomatal conductance reduction [Figure 4A]).

In contrast to our experimental data (Figure 4), Stomata 2.0 predicted identical conductance levels for low and high CO₂ concentration in the absence of ABA (Figure 3B). In an illustration of the use of Boolink, we modified the ABA network further, with as goal to incorporate CO₂ dependence on steady-state conductance levels when ABA is absent. Creating this updated network, Stomata 2.1, was greatly facilitated by the ability of Boolink to easily implement changes and generate predictions. We introduced CO₂ dependence on calcium signaling based on experimental evidence that Ca2c is involved in CO₂-induced stomatal closure (Schwartz et al., 1988; Schulze et al., 2021; Webb et al., 1996). Furthermore, it is well-established that anion efflux and water efflux from guard cells are essential for the CO2induced reduction in stomatal conductance. Furthermore, findings that GHR1 functions in CO2-induced stomatal closure (Hõrak et al., 2016; Jakobson et al., 2016) were expanded to include GHR1 predictions of the original ABA signaling model (Albert et al., 2017). Addition of an ABA component to microtubule function was motivated based on recent findings on roles of guard cell microtubules (Qu et al., 2018; Rui and Anderson, 2016). The output of Stomata 2.1 was able to better incorporate effects of CO₂ and the present experimental data (Figure 5B). As described

earlier, important gaps exist in the understanding of the CO_2 signaling pathway, including that the primary CO_2 or bicarbonate sensors remain unknown in guard cells and the mechanisms by which HT1, CBC1, and CBC2 link to one another and to stomatal closing mechanisms are unknown. Expansion of the present model will be required.

In the present study, ABA responses were analyzed at near-zero CO₂ in the C3 model plant Arabidopsis. The robust decrease of steady-state stomatal conductance at near-zero CO2 by ABA addition was also found in the C3 species such as Oats (Avena sativa), Cotton (Gossypium hirsutum), and Cocklebur (Xanthium strumarium) but was not found in the C4 species such as Amaranth (Amaranthus powellii) and Maize (Zea mays; Dubbe et al., 1978), suggesting a species variability in the response. The converse response was also analyzed in which CO2 responses were observed in the absence of exogenously added ABA in these C3 and C4 species (Dubbe et al., 1978). Interestingly, a variation among species was detected, in which either CO2 responses proceeded in the C4 species or were impaired in the C3 species (Dubbe et al., 1978). These findings are consistent with recent findings that CO₂ signaling requires basal ABA signaling and would be predicted to depend on variation in basal levels of ABA in guard cells depending on plant species and growth conditions (Hsu et al., 2018; Zhang et al., 2020). These classical findings (Dubbe et al., 1978; Raschke, 1975) corresponds to a model in which ABA and basal ABA signaling plays an important role for other stomatal closing stimuli.

Our proposed additions to the existing ABA network, which illustrate the potential use of Boolink, are meant as a starting point for further explorations, and further research is needed to determine the precise mechanism by which CO₂ signaling merges with ABA signal transduction. Nevertheless, several improvements can be suggested. First, it is conceivable that CO₂ affects yet unknown mechanisms. Second, the CO₂ pathway may contain feedback loops, which can be easily implemented within Boolink (Figure 1;Dubbe et al., 1978). Finally, we should point out that Boolean networks do not incorporate explicit rate constants and contain nodes that can only take one of two values (0 or 1). Therefore, these networks are not able to address the time dependence of responses nor how they respond to graded inputs.

Importantly, the GUI platform and stomatal signaling model we developed can be used and altered by the public community of users to generate diverse testable predictions to add expanded components, or to modify the ABA and CO₂ signaling models. Furthermore, the methods and openaccess software tools we have presented can be of interest to the wider life sciences and plant biology community interested in physiological pathways.

Materials and methods

Software

Boolink is implemented using Python and C++ and can be freely downloaded from the GitHub repository (https://

github.com/dyhe-2000/Boolink-GUI and https://github.com/Rappel-lab/Boolink-GUI). It requires a current version of Python and C++ and a detailed manual, including installation instructions, is provided in the GitHub repository. These instructions are provided for Windows, Mac, or Linux-based computers. Boolink can also be run as a Docker container, a self-contained environment that includes all the required packages and utilities, on MacOS and Linux-based systems. The advantage of this method is that users only need to install the desktop client for Docker and not the dependencies like C++ and Python. A detailed explanation of instructions to install the Docker client and the required script to run the container are given in the Supplementary data and in the GitHub repository.

Experiments

Plants of the Arabidopsis (A. thaliana) accession Columbia (Col-0) were grown as described by Hsu et al. (2018). Stomatal conductance measurements in response to ABA were performed in detached intact leaves of 5.5- to 7-weekold plants in Arabidopsis leaves following the procedure described previously (Ceciliato et al., 2019) using a LI-6800 Portable Photosynthesis System with an integrated Multiphase Flash Fluorometer (6800-01A; LI-COR Biosciences, Lincoln, Nebraska, USA). Detached leaves were clamped in the leaf chamber and kept at \sim 1.5 ppm or 400 ppm CO_2 , 135 μ mol m⁻² s⁻¹ red light combined with 15 $\mu \text{mol m}^{-2} \text{ s}^{-1}$ blue light, $70 \pm 0.5\%$ or $65 \pm 0.5\%$ relative air humidity, 21°C heat exchanger temperature, and 500 μmol·s⁻¹ incoming air flow rate for at least 2 h until stomatal conductance equilibrated and stabilized. Stomatal conductances were recorded every 30 s under ∼1.5-ppm or 400-ppm CO₂ for 10 min. ABA (2 μM) was then added to the transpiration stream via the petiole, and stomatal conductances were recorded as shown in the figures. In each independent set of experiments, intact leaves from independent plants were analyzed per experimental condition.

Supplemental data

The following materials are available in the online version of this article.

Supplemental Text. Contains a primer on Boolean logic, details of Stomata 2.1, and installation and operating instructions of Boolink.

Funding

This research was funded by a grant from the National Science Foundation (MCB-1900567) to W.J.R. and J.I.S. S.S. was supported by a Deutsche Forschungsgemeinschaft (DFG) fellowship (SCHU 3186/1-1:1). G.D. was supported by an EMBO long-term post-doctoral fellowship (ALTF334-2018).

Conflict of interest statement. No conflict of interest.

References

- Albert I, Thakar J, Li S, Zhang R, Albert R (2008) Boolean network simulations for life scientists. Source Code Biol Med 3: 1–8
- Albert R, Acharya BR, Jeon BW, Zañudo JG, Zhu M, Osman K, Assmann SM (2017) A new discrete dynamic model of ABA-induced stomatal closure predicts key feedback loops. PLoS Biol 15: e2003451
- Bock M, Scharp T, Talnikar C, Klipp E (2014) BooleSim: an interactive Boolean network simulator. Bioinformatics 30: 131–132
- **Bornholdt S** (2008) Boolean network models of cellular regulation: prospects and limitations. J Royal Soc Interface **5**: S85–S94
- Brodland GW (2015) How computational models can help unlock biological systems. Semin Cell Dev Biol 47-48: 62–73
- Ceciliato PH, Zhang J, Liu Q, Shen X, Hu H, Liu C, Schäffner AR, Schroeder JI (2019) Intact leaf gas exchange provides a robust method for measuring the kinetics of stomatal conductance responses to abscisic acid and other small molecules in Arabidopsis and grasses. Plant Methods 15: 1–10.
- Dahlhaus M, Burkovski A, Hertwig F, Mussel C, Volland R, Fischer M, Debatin KM, Kestler HA, Beltinger C (2016) Boolean modeling identifies Greatwall/MASTL as an important regulator in the AURKA network of neuroblastoma. Cancer Lett 371: 79–89
- Di Cara A, Garg A, De Micheli G, Xenarios I, Mendoza L (2007)

 Dynamic simulation of regulatory networks using SQUAD. BMC

 Bioinfor 8: 1–10
- Dimitrova E, García-Puente LD, Hinkelmann F, Jarrah AS, Laubenbacher R, Stigler B, Stillman M, Vera-Licona P (2011)

 Parameter estimation for Boolean models of biological networks.

 Theor Comp Sci 412: 2816–2826
- **Dubbe DR, Farquhar GD, Raschke K** (1978) Effect of abscisic acid on the gain of the feedback loop involving carbon dioxide and stomata. Plant Physiol **62**: 413–417
- Feist AM, Henry CS, Reed JL, Krummenacker M, Joyce AR, Karp PD, Broadbelt LJ, Hatzimanikatis V, Palsson BØ (2007) A genome-scale metabolic reconstruction for Escherichia coli K-12 MG1655 that accounts for 1260 ORFs and thermodynamic information. Mol Sys Biol 3: 121
- Garg A, Di Cara A, Xenarios I, Mendoza L, De Micheli G (2008) Synchronous versus asynchronous modeling of gene regulatory networks. Bioinformatics 24: 1917–1925
- **Genoud T, Métraux JP** (1999) Crosstalk in plant cell signaling: structure and function of the genetic network. Trend Plant Sci 4: 503–507
- Gonzalez AG, Naldi A, Sanchez L, Thieffry D, Chaouiya C (2006) GINsim: a software suite for the qualitative modelling, simulation and analysis of regulatory networks. Biosystems 84: 91–100
- Hashimoto M, Negi J, Young J, Israelsson M, Schroeder JI, Iba K (2006) Arabidopsis HT1 kinase controls stomatal movements in response to CO 2. Nat Cell Biol 8: 391–397
- Helikar T, Kowal B, McClenathan S, Bruckner M, Rowley T, Madrahimov A, Wicks B, Shrestha M, Limbu K, Rogers JA (2012) The cell collective: toward an open and collaborative approach to systems biology. BMC Sys Biol 6: 1–14
- Helikar T, Rogers JA (2009) ChemChains: a platform for simulation and analysis of biochemical networks aimed to laboratory scientists. BMC Syst Biol 3: 1–15
- Herrmann F, Groß A, Zhou D, Kestler HA, Kühl M (2012) A Boolean model of the cardiac gene regulatory network determining first and second heart field identity. PloS One 7: e46798
- Hills A, Chen ZH, Amtmann A, Blatt MR, Lew VL (2012) OnGuard, a computational platform for quantitative kinetic modeling of guard cell physiology. Plant Physiol 159: 1026–1042
- Hiyama A, Takemiya A, Munemasa S, Okuma E, Sugiyama N, Tada Y, Murata Y, Shimazaki KI (2017) Blue light and CO 2 signals converge to regulate light-induced stomatal opening. Nature Comm 8: 1–13

- Hõrak H, Sierla M, Tõldsepp K, Wang C, Wang YS, Nuhkat M, Valk E, Pechter P, Merilo E, Salojärvi J, et al. (2016) A dominant mutation in the HT1 kinase uncovers roles of MAP kinases and GHR1 in CO2-induced stomatal closure. Plant Cell 28: 2493–2509
- Hsu PK, Takahashi Y, Munemasa S, Merilo E, Laanemets K, Waadt R, Pater D, Kollist H, Schroeder JI (2018) Abscisic acid-independent stomatal CO2 signal transduction pathway and convergence of CO2 and ABA signaling downstream of OST1 kinase. Proc Natl Acad Sci U S A 115: E9971–E9980
- Hu H, Boisson-Dernier A, Israelsson-Nordström M, Böhmer M, Xue S, Ries A, Godoski J, Kuhn JM, Schroeder JI (2010) Carbonic anhydrases are upstream regulators of CO 2-controlled stomatal movements in guard cells. Nat Cell Biol 12: 87–93
- Hu H, Rappel WJ, Occhipinti R, Ries A, Böhmer M, You L, Xiao C, Engineer CB, Boron WF, Schroeder JI (2015) Distinct cellular locations of carbonic anhydrases mediate carbon dioxide control of stomatal movements. Plant Physiol 169: 1168–1178
- Hua D, Wang C, He J, Liao H, Duan Y, Zhu Z, Guo Y, Chen Z, Gong Z (2012) A plasma membrane receptor kinase, GHR1, mediates abscisic acid-and hydrogen peroxide-regulated stomatal movement in Arabidopsis. Plant Cell 24: 2546–2561
- **Hundt R** (2011) Loop recognition in C++/java/go/scala *In* Proceedings of Scala Days, Stanford, 2011. https://days2011.scalalang.org/sites/days2011/files/ws3-1-Hundt.pdf
- **Irons D** (2009) Logical analysis of the budding yeast cell cycle. J Theor Biol **257**: 543–559
- Jakobson L, Vaahtera L, Tõldsepp K, Nuhkat M, Wang C, Wang YS, Hõrak H, Valk E, Pechter P, Sindarovska Y, et al. (2016) Natural variation in Arabidopsis Cvi-0 accession reveals an important role of MPK12 in guard cell CO2 signaling. PLoS Biol 14: e2000322
- Kauffman SA (1969) Metabolic stability and epigenesis in randomly constructed genetic nets. J Theor Biol 22: 437–467
- **Kime CR, Mano MM** (2003) Logic and Computer Design Fundamentals. Prentice Hall, Hoboken, New Jersey.
- Klamt S, Saez-Rodriguez J, Gilles ED (2007) Structural and functional analysis of cellular networks with CellNetAnalyzer. BMC Sys Biol 1: 1–13
- **Klarner H, Streck A, Siebert H** (2017) PyBoolNet: a python package for the generation, analysis and visualization of Boolean networks. Bioinformatics **33**: 770–772
- **Lau KY, Ganguli S, Tang C** (2007) Function constrains network architecture and dynamics: A case study on the yeast cell cycle Boolean network. Phys Rev E **75**:051907
- **Li F, Long T, Lu Y, Ouyang Q, Tang C** (2004) The yeast cell-cycle network is robustly designed. Proc Natl Acad Sci U S A **101**: 4781–4786
- Li S, Assmann SM, Albert R (2006) Predicting essential components of signal transduction networks: a dynamic model of guard cell abscisic acid signaling. PLoS Biol 4: e312
- Maheshwari P, Assmann SM, Albert R (2020) A guard cell abscisic acid (ABA) network model that captures the stomatal resting state. Front Physiol 11: 927
- Maheshwari P, Du H, Sheen J, Assmann SM, Albert R (2019) Model-driven discovery of calcium-related protein-phosphatase inhibition in plant guard cell signaling. PLoS Computat Biol 15: e1007429.
- Melke P, Jönsson H, Pardali E, ten Dijke P, Peterson C (2006) A rate equation approach to elucidate the kinetics and robustness of the TGF-β pathway. Biophys J 91: 4368–4380
- Merilo E, Jalakas P, Kollist H, Brosché M (2015) The role of ABA recycling and transporter proteins in rapid stomatal responses to reduced air humidity, elevated CO2, and exogenous ABA. Mol Plant 8: 657–659
- Merilo E, Laanemets K, Hu H, Xue S, Jakobson L, Tulva I, Gonzalez-Guzman M, Rodriguez PL, Schroeder JI, Brosche M, et al. (2013) PYR/RCAR receptors contribute to ozone-, reduced air

- humidity-, darkness-, and CO2-induced stomatal regulation. Plant Physiol **162**: 1652–1668
- Muraro D, Byrne H, King J, Voß U, Kieber J, Bennett M (2011)
 The influence of cytokinin–auxin cross-regulation on cell-fate determination in Arabidopsis thaliana root development. J Theor Biol 283: 152–167
- Müssel C, Hopfensitz M, Kestler HA (2010) BoolNet—an R package for generation, reconstruction and analysis of Boolean networks. Bioinformatics 26: 1378–1380
- Paulevé L (2017) Pint: a static analyzer for transient dynamics of qualitative networks with IPython Interface. International Conference on Computational Methods in Systems Biology. Springer, pp 309–316
- Phillips R (2015) Theory in biology: figure 1 or figure 7? Trends Cell Biol 25: 723–729
- **Prechelt L** (2000) An empirical comparison of seven programming languages. Computer **33**: 23–29
- Qu Y, Song P, Hu Y, Jin X, Jia Q, Zhang X, Chen L, Zhang Q (2018) Regulation of stomatal movement by cortical microtubule organization in response to darkness and ABA signaling in Arabidopsis. Plant Growth Regul 84: 467–479
- Raschke K (1975) Simultaneous requirement of carbon dioxide and abscisic acid for stomatal closing in Xanthium strumarium L. Planta 125: 243–259
- Rui Y, Anderson CT (2016) Functional analysis of cellulose and xyloglucan in the walls of stomatal guard cells of Arabidopsis. Plant Physiol 170: 1398–1419
- Schulze S, Dubeaux G, Ceciliato PH, Munemasa S, Nuhkat M, Yarmolinsky D, Aguilar J, Diaz R, Azoulay-Shemer T, Steinhorst L, Offenborn JN, et al. (2021) A role for calcium-dependent protein kinases in differential CO2-and ABA-controlled stomatal closing and low CO2-induced stomatal opening in Arabidopsis. New Phytol 229: 2765–2779
- Schwab JD, Kestler HA (2018) Automatic screening for perturbations in Boolean networks. Front Physiol 9: 431
- Schwab JD, Kühlwein SD, Ikonomi N, Kühl M, Kestler HA (2020) Concepts in Boolean network modeling: What do they all mean? Comput Struct Biotechnol J 18: 571–582
- Schwartz A, Ilan N, Grantz DA (1988 Calcium effects on stomatal movement in Commelina communis L.: use of EGTA to modulate stomatal response to light, KCl and CO₂. Plant Physiol **87**: 583–587
- Shou W, Bergstrom CT, Chakraborty AK, Skinner FK (2015) Theory, models and biology. eLife 4: e07158
- Sierla M, Hõrak H, Overmyer K, Waszczak C, Yarmolinsky D, Maierhofer T, Vainonen JP, Salojärvi J, Denessiouk K,

- **Laanemets K**, **et al.** (2018) The receptor-like pseudokinase GHR1 is required for stomatal closure. Plant Cell **30**: 2813–2837
- Stoll G, Viara E, Barillot E, Calzone L (2012) Continuous time Boolean modeling for biological signaling: application of Gillespie algorithm. BMC Sys Biol 6: 1–18
- Terfve C, Cokelaer T, Henriques D, MacNamara A, Goncalves E, Morris MK, van Iersel M, Lauffenburger DA, Saez-Rodriguez J (2012) CellNOptR: a flexible toolkit to train protein signaling networks to data using multiple logic formalisms. BMC Systems Biol 6: 1–14
- **Timmermann T, González B, Ruz GA** (2020) Reconstruction of a gene regulatory network of the induced systemic resistance defense response in Arabidopsis using Boolean networks. BMC Bioinformatics **21**: 1–16
- Waidyarathne P, Samarasinghe S (2018) Boolean calcium signalling model predicts calcium role in acceleration and stability of abscisic acid-mediated stomatal closure. Sci Rep 8: 1–16
- Wang RS, Saadatpour A, Albert R (2012) Boolean modeling in systems biology: an overview of methodology and applications. Phy Biology 9:055001
- Wang Y, Hills A, Vialet-Chabrand S, Papanatsiou M, Griffiths H, Rogers S, Lawson T, Lew VL, Blatt MR (2017) Unexpected connections between humidity and ion transport discovered using a model to bridge guard cell-to-leaf scales. Plant Cell 29: 2921–2939
- Webb AA, McAinsh MR, Mansfield TA, Hetherington AM (1996)
 Carbon dioxide induces increases in guard cell cytosolic free calcium. Plant J 9: 297–304
- Xue S, Hu H, Ries A, Merilo E, Kollist H, Schroeder JI (2011)
 Central functions of bicarbonate in S-type anion channel activation and OST1 protein kinase in CO2 signal transduction in guard
 cell. EMBO J 30: 1645–1658
- Zhang H, Lin M, Shi H, Ji W, Huang L, Zhang X, Shen S, Gao R, Wu S, Tian C (2014) Programming a Pavlovian-like conditioning circuit in Escherichia coli. Nature Commun 5: 1–10
- Zhang J, De-oliveira-Ceciliato P, Takahashi Y, Schulze S, Dubeaux G, Hauser F, Azoulay-Shemer T, Tõldsepp K, Kollist H, Rappel WJ, et al. (2018) Insights into the molecular mechanisms of CO2-mediated regulation of stomatal movements. Curr Biol 28: R1356–R1363
- Zhang L, Takahashi Y, Hsu PK, Kollist H, Merilo E, Krysan PJ, Schroeder JI (2020) FRET kinase sensor development reveals SnRK2/OST1 activation by ABA but not by MeJA and high CO2 during stomatal closure. eLife 9: e56351
- Zheng J, Zhang D, Przytycki PF, Zielinski R, Capala J, Przytycka TM (2010) SimBoolNet—a Cytoscape plugin for dynamic simulation of signaling networks. Bioinformatics 26: 141–142